Function through Defects : Thermodynamics and Kinetics of Point Defects in Ionic Solids

Joachim Maier

Max-Planck-Institut für Festkörperforschung, Heisenbergstraße 1,
D-70569 Stuttgart, Germany
(Received October 2, 1997)

The significance of point defects as relevant centers concerning electrochemical function is highlighted. Starting from the most simple case of dilute equilibrium bulk defect chemistry, influence of defect interaction and in particular the impact of interfaces on point defect redistribution are considered. Then recent progress in the field of kinetics in bulk and at boundaries is discussed. Finally, selected applications with emphasis on battery and sensor technology are presented.

Key words : Electroceramics, Thermodynamics, Kinetics. Interfaces, Transport

I. Introduction : The Significance of Point Defects in Solids

The two best understood materials in our world are -- in regard to the electrical properties -- the chemist's water and the physicist's silicon. In both cases, however, it is not the (hypothetical) perfect state -- so-to-speak the chemical ground state of solids -- which is of prime interest. Rather, the deviations, so-to-speak the chemical excitations, do cause the electrical and electrochemical functions : In pure water this role is played by the H_3O^+- and OH^--ions, in pure silicon by the conduction-electrons and electron holes; generally speaking excess and deficient particles, and in addition foreign particles have to be considered (see Fig. 1).

In ionic crystals, ionic and electronic defects are simultaneously present in varying concentrations, while the regular ions are immobilised by virtue of the lattice energy (relative charge is zero) the point defects are more or less mobile. The resulting conductivity is crucial to the electric properties but also for mass transport and chemical reaction kinetics; consider e.g. the mechanisms of chemical synthesis, of sintering or of corrosion [1]. Whilst point defects such as interstitial particles, vacancies, substitutional ions, excess and defect electrons also exist in thermodynamic equilibrium as a consequence of the pronounced configurational entropy, this is (in all cases of interest) not the case for the higher-dimensional defects such as dislocations or grain boundaries. In view of the frequently pronounced metastability of the two- (or even three-) dimensional defects, they nevertheless play a fundamental role in real materials due to both their structure (core region) and the point defect redistribution in the spatial regions adjacent (space charge layers). A special role is played by phase boundaries such as surfaces. the sheer existence of which may be required by mass conservation. But also then the morphology involved is usually not the equilibrium morphology due to kinetic constraints. Parallel and perpendicular to the higher-dimensional defects the electrical function is often significantly modified.
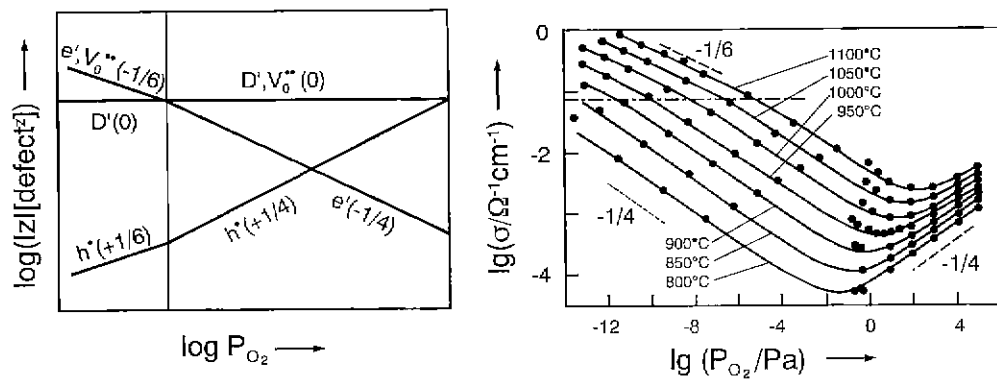
II. Equilibrium Concentration of Point Defects in Bulk and Near Interfaces

1. Bulk

In most materials the point defect concentrations are
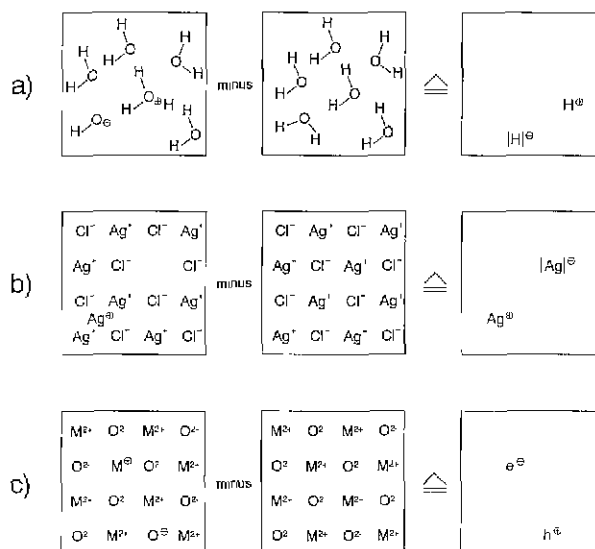
Fig. 1. Isomorphism of the "internal chemistry" of solids as the basis of the dynamics of ceramic processes and functions in comparison with the internal acid-base chemistry of water [1].

Fig. 2. The dependence of the charge carrier concentrations in acceptor-doped $SrTiO_3$ derived from Eq. (1) (l. h. s.) is in complete agreement with the conductivity experiments [4].

so small that approximately Boltzmanns distribution is valid. In those cases the defect reactions (e.g. the ones indicated in Fig. 1) can be treated by ideal mass action laws [2]. In the case of a simple defect chemistry the concentration of each carrier (c_i) in the compound MX (and thus the precise thermodynamic state) is obtained as a function of temperature (T), of the chemical environment (component chemical potential, expressed by the partial pressure P of X_2) and the effective doping level (C) as [3,1]

$$c_i(T, P, C) = \alpha_j \, P^{N_j} \, C^{M_j} \, \Pi_l \, K_l^{r_{lj}}(T) \qquad (1)$$

If the compound is multinary, further component partial pressures need to be fixed. Usually, however, not all interactions with the environment are reversible; e.g. for T < 1000 K the Sr/Ti ratio in $SrTiO_3$ is frozen-in and the compound is pseudo-binary. Then the concentration of the Sr-defects can be treated as a constant (determined by preparation) and only enters the C-term in Eq. (1). On the other hand, in many oxides also protonic defects can be reversibly incorporated or ex-corporated [8]. Thus, in Yb-doped $BaCeO_3$, besides T, [Yb] and P_{O_2} also P_{H_2O} (or P_{H_2}) have to be defined. The figures 2, 4 which will not be discussed in detail shall give examples with respect to bulk analysis for $SrTiO_3$ and $(La, Sr)_2CuO_4$.

The figures 2, 4 do not only show that the defect concentrations can be calculated in ionic conductors, mixed conductors, high temperature superconductors, but also how subtly they can be varied. The profoundness of the basic understanding in electroceramics is in many cases certainly comparable with the one in Si or H_2O, moreover, the complexity is increased especially because of the simultaneous presence of ionic and electronic carriers. Fig. 2 indicates how sensitive the charge carrier concentrations in $SrTiO_3$ depend on P_{O_2} and thus on nonstoichiometry. At low P_{O_2} reduced states ($Ti^{3+} \hat{=} e'$) are important. On increasing P_{O_2}, oxygen is incorporated in vacancies and conduction electrons are annihilated, the electronic conductivity decreases, until, on further increase, holes as new carriers are generated (formation of O) [9]. The absolute value of $[V_O^{\cdot\cdot}]$ changes adequately, the relative change, however, is tiny and negligible.

The defect chemistry of the high temperature superconductors explains the effects of temperature, doping and oxygen partial pressure on the concentration of holes which are essential for superconductivity, as well as of oxygen defects which are decisive for the preparation, processing and annealing kinetic. It must of course not be overlooked that the concentrations at low
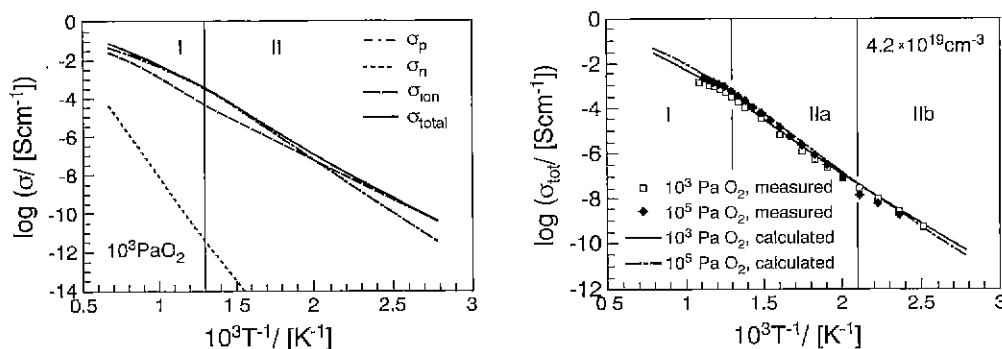
Fig. 3. The calculation of the specific conductivity of ions and electrons according to the mass action formalism for Fe-doped $SrTiO_3$ ([Fe] = 4.2 × 10^{19} cm^{-3}; P_{O_2} = 10^3 Pa) exactly reflects the measured conductivities, if the experimentally known T-dependent mobilities are taken account of and if the freezing of the surface reaction is considered [5].
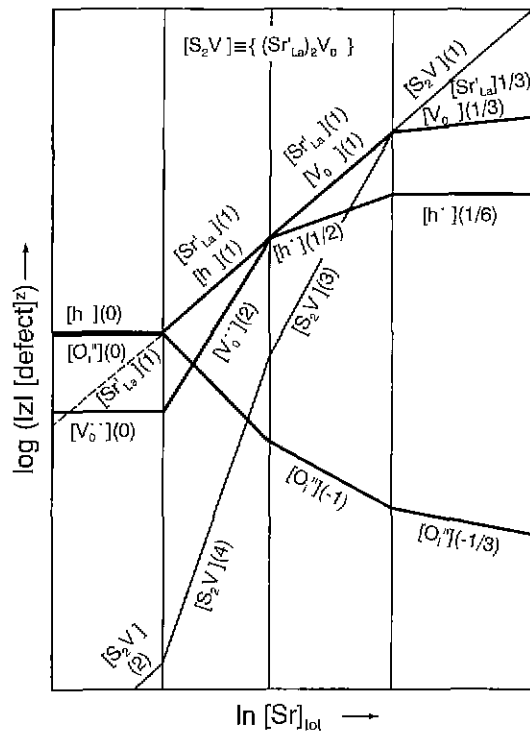
Fig. 4. Doping dependence of the charge carrier concentrations in the $(La, Sr)_2CuO_4$ high T_c superconductor [6].

temperatures are not identical with the values at high T, even not if quenching occurred very rapidly, since fast electronic equilibria and ordering phenomena have to be paid attention to. Finally, the formation of Cooper-pairs itself represents a (e.g., phonon-assisted) association reaction becoming significant only at the critical temperature.

Interactions also become important at high carrier concentrations. Short range interaction can often be successfully taken into account by introducing associates, while long range order effects may be tackled by the Debye-Hückel-theory [10]. In different cases a cube root law seems to be an adequate description reflecting a simple Madelung interaction in a mean field sense [11].

2. At Boundaries

Near boundaries the electroneutrality condition has to be replaced by Poisson's equation. Due to the modified structure of the boundary core itself (or of the neighbouring phase), a preferential carrier segregation (redistribution) occurs resulting in a charge separation. As extent and extension are strongly limited by the accompanying electric fields, the effects on charge carrier concentration and conductivity can be drastic [7]. Conceptionally one might actually speak of heterogeneous doping if this effect is used by intentional introduction of interfaces (e.g. by admixing insoluble second phases) as displayed in Fig. 5. The width of the space charge layer is roughly given by the Debye-length which sensitively depends on the bulk defect concentrations as

$$\frac{c_j}{c_{j\infty}} = \left[\frac{1 + \vartheta_j \exp - (x/\lambda)}{1 - \vartheta_j \exp - (x/\lambda)} \right]^2 \tag{2}$$

(The index ∞ refers to the bulk.)

III. Electrical Conductivity Effects

1. In the Bulk

In isotropic media the specific conductivity (σ) is given by the product of charge, concentration and mobility. While the first quantity has been analysed above and its temperature dependence has been shown to be given by the relevant formation enthalpy of the defects, the last quantity is, in the case of ions, proportional to the rate constant of the process of hopping from one to the next equivalent lattice site and thus essentially determined by the free activation enthalpy of that process. (This is similar for polarons. Free electrons (or holes) are essentially de-accelerated by phonon scattering.) As far as σ is concerned, also the relevant free defect formation enthalpy is essential, as analysed above.

Deviations from this simple picture appear in boundary regions, in anisotropic solids, at high defect concentrations and under high fields [11].

How detailed the defect chemistry is able to predict conductivity effects is shown in Figs. 2, 3. High field effects lead to deviations from the linear response behaviour and can result in qualitative changes of properties and morphologies [1]. It is worth mentioning that volta-
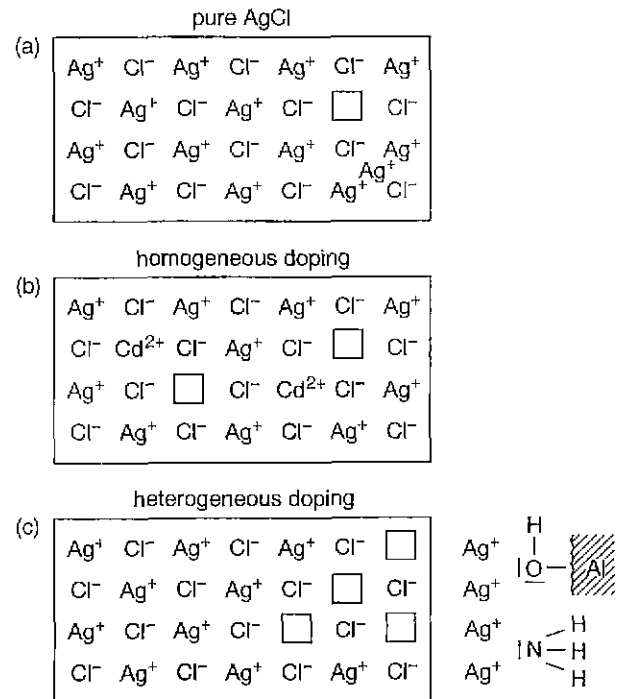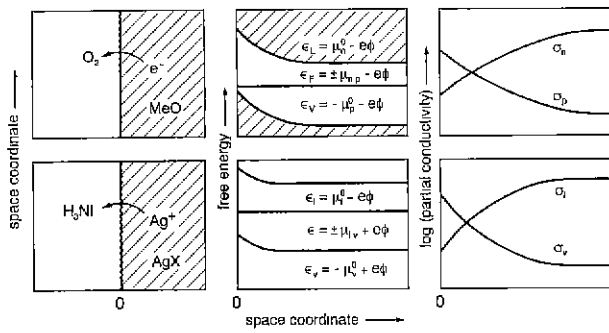

Fig. 5. The introduction of interfaces leads to effects which are analogous to homogeneous doping in many respects [7].

Fig. 6. Acid-base-active gases can produce ionic space charge regions at the interface in the same way as redox-active gases produce electronic effects [7]. This can be applied in gas sensors.

ges of a few volts may lead to decomposition phenomena.

2.Perpendicular through Boundaries

Interfaces as they may be formed between grains in ceramics or between a solid and an electrode, may cause additional resistances: (i) transfer resistances (in the case of gas electrodes, e.g., these quantities usually characterise a complex scheme of elementary reaction steps), (ii) resistance due to composition changes during current flow and (iii) resistances due to depletion layers which may already exist in equilibrium. In the last case one obtains for the effective specific excess resistance.

$$\Delta \rho_m^{\perp} \propto \frac{\lambda}{u_j c_{j\infty}} \frac{|\vartheta_j|}{1+\vartheta_j} \tag{3}$$

A detailed treatment is given in Ref. [7]. A fourth and frequently met type of interfacial resistance stems from current constriction phenomena [12]. Prominent examples are impedance effects of porous solids, composites or resistances stemming from laterally inhomogeneous grain boundaries [13].

3. Along and Parallel to the Interface
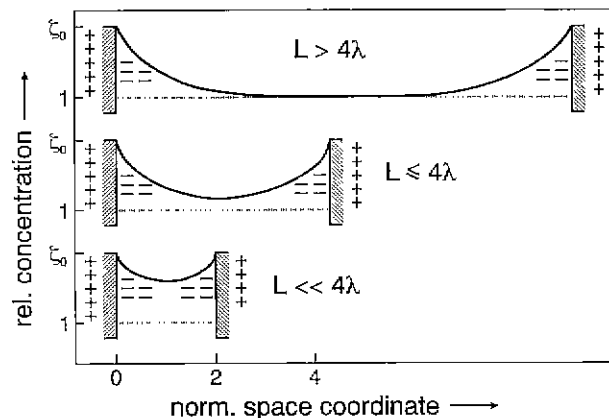
Fig. 7. When the sample thickness becomes comparable to the space charge thickness, then a mesoscopic effect occurs [7].

Interfaces can also provide fast pathways [7] along the structurally different core or -- especially in weakly disordered compounds with mobile defects -- along space charge regions (enrichment layers). A variety of conductivity anomalies at boundaries involving ionic conductors can be explained in this way [7] (s. Fig. 5).

In turn the space charge effects at grain boundaries can be tailored by introducing charge carrier sources or sinks. Examples are the contamination of AgCl-grain boundaries with NH_3 (s. Fig 6) or of CaF_2-grain boundaries with BF_3 or SbF_5 [7].

These Lewis bases or acids are effective attractors for the mobile Ag^+ or F^--ions. In this way the respective vacancy concentration is significantly increased in the space charge layer adjacent [7]. Completely analogous to that is the influencing of electronic carriers by redox-active grain boundaries or corresponding grain boundary modification. The conductivity increase can be calculated as

$$\Delta \sigma_m^{||} \propto \lambda u_j c_{j\infty} \frac{\vartheta_j}{1-\vartheta_j} \tag{4}$$

4. Superposition of Serial and Parallel Pathways

In real polycrystalline or composite ceramics serial and parallel effects are superimposed. In the case of simple microstructures it was possible to analyse this situation by impedance spectroscopy and to separate the conductivity mechanisms (AgCl/AgCl; AgCl/Al$_2$O$_3$; AgCl/AgI [7,14]).

In the case of complex microstructures the treatment of these phenomena is highly involved even if only one mechanism is decisive and requires percolation or effective medium [5] calculations, or finite element computations [15]. In AgCl: AgI composites e.g. the ionic conductivity $(T < T_{\alpha\beta})$ is dominated by pathways which them-
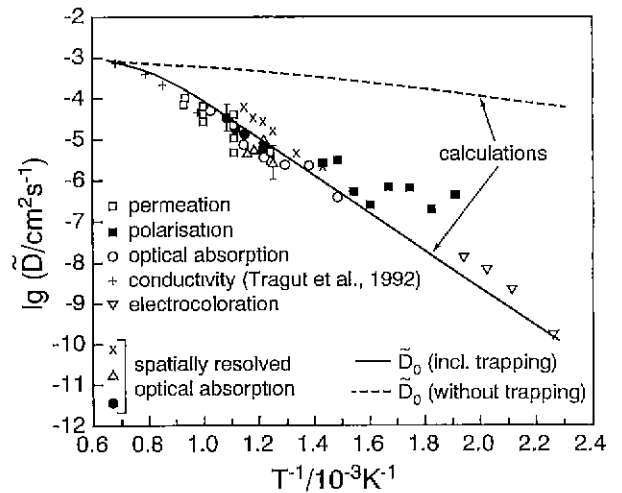
Fig. 8. Chemical diffusion coefficient of oxygen in Fe-doped SrTiO$_3$ measured by a variety of independent methods. The solid line indicates the prediction according to the theoretical treatment which includes trapping phenomena.

selves consist of hetero- and homo-junctions. At high temperatures ($T > T_{\alpha\beta}$), AgI exists in its super-ionic α-form, the ionic transport occurs via the α-AgI grains and follows a percolation law [16].

5. Nano-systems

Nanocrystalline solids are of special importance in this context. Not only is the fraction of the interfaces and of triple or quadruple junctions increased, but also qualitative differences to micro-polycrystalline samples do appear. From cluster chemistry it is shown that the bulk structure is reached at already small crystal sizes in many examples of interest. However, the space charge layers interfere when the sample size is comparable to the space charge layer width (Fig. 7). Conductivity enhancement effects, in addition to Eq. (4), caused by this phenomenon can be described by a nano-size factor [7,17] which is given by

$$\text{Nano} - \text{size} - \text{factor} = \frac{4\lambda}{L} \left[\frac{c_0 - c^*}{c_0} \right]^{1/2} \qquad (5)$$

(λ : Debye-length, L : sample size, c_0 : interface concentration, c^* : concentration in the grains center ($L/2$), c^* is implicitly correlated with L and c_0 in a complicated but defined way as shown in Refs. [7,17])

IV. Chemical Kinetics

Chemical kinetics and mass transport play a decisive role during preparation (synthesis, sintering) as well as for the degradation and corrosion of materials but also for the performance (transformation of chemical into electrical signals). Again, point defects (besides higher dimensional defects) are the relevant mechanistic centers [18].
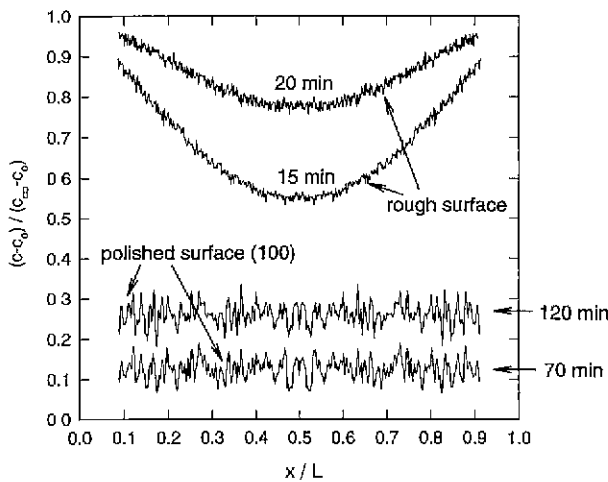
Fig. 9. Concentration distribution as a function of space and time derived from the optical technique in-situ, top: diffusion control; bottom: surface control; SrTiO$_3$ single crystal, $T = 650°C$, $m_{Fe} = 4.6 \times 10^{19}$cm^{-3}.

As a master example we discuss the oxygen incorporation/ex-corporation of an oxide (SrTiO$_3$), as it is relevant to bulk conductivity sensors (cf. response time) or the conditioning of high temperature superconductors.

For the purpose of simplicity, in the following we subsume the complex elementary steps on the surface under the name "interfacial reaction" : This step is in series to the chemical diffusion which, in our case, is an ambipolar diffusion of O^{2-} and 2e$^-$ (e.g. O$_i''$ and 2h$^{\cdot}$). The corresponding diffusion coefficient is composed of the individual diffusion coefficients of the ionic and electronic defects [19]. In the case of internal redox reactions the situation is more complicated. In the case of valence changes of the oxygen ion being in local equilibrium, the chemical diffusion coefficient reads [20]

$$\widetilde{D} \propto [2\sigma_1 + 4s + (\sigma_{eon} - \sigma_1)(\sigma_2 + \sigma_1)/\sigma]$$

$$\left[\frac{\chi_{12}}{c_{12}} + \frac{4\chi_{21}}{c_{21}} \right] \propto [\widetilde{\sigma}] \cdot [\widetilde{c}^{-1}] \qquad (6)$$

(σ_2, σ_1 : conductivities of O^{2-}, O$^-$; χ : trapping factor which has (without restriction of generality) been evaluated in Eq.(6) in terms of O$_i''$(i2) and e'(n)).

In the case of SrTiO$_3$ in-diffusion at high temperatures could be made visible as a function of space and time by an optical absorption technique [21]. The diffusion data obtained can be only understood -- but then with an excellent precision -- if the influence of redox-active impurities is taken into account in the kinetics [22] (s. Fig. 8). They are essentially immobile and only act on the ambipolar conductivity via their influence in the electroneutrality equation (doping effect), but are (even if negligible in the electroneutrality equation) of high significance for the ambipolar concentration $\widetilde{c}$. Exactly that case is met in the Y-doped ZrO$_2$, the classical solid electrolyte in HT-fuel cells [23]. Redox-active impurities such as Ni or Ti do not influence conductivities and concentrations as shown by Eq. (1) in which $C \approx [Y'_{Zr}] >> [Ti'_{Zr}]$ etc. as long as the oxygen interaction equilibrium is established. However, they are of fundamental importance for $\widetilde{D}$ as calculations and experiments show, and are responsible for the large scatter in literature as well as for the steep T-dependence. Exactly this can be understood by the kinetic redox effect [20]. The deeper reason lies in the availability of trapped carriers via local equilibrium. Most active are mid-gap impurities.

Chemical transport through and along grain boundaries is of major practical importance. Recently we analysed the transport through grain boundaries indicating space charge regions [24]. In this context we only give a limiting result which is valid in many cases. If the interfacial density is not too high and the grain boundaries are blocking, then it can be shown that $\widetilde{\sigma}$ is determined by the grain boundaries, while the stoichiometry change ($\widetilde{c}$) mainly affects the bulk, such that

$$\tilde{D} \propto \frac{l}{d} \frac{\tilde{\sigma}_{gb}}{\tilde{c}_{bulk}} \qquad (7)$$

The scaling factor l/d is the ratio of grain size and grain boundary width.

The diffusion along boundaries (see e.g. Ref. [25]) is already involved in the absence of space charges, since gradients perpendicular to the boundaries appear during the process widening the effective boundary path continuously. Only if grain boundary diffusion is extremely fast, a simple well-known relation is valid, viz.

$$\tilde{D}_m \propto \frac{L^2}{l^2} \frac{\tilde{\sigma}_{bulk}}{\tilde{c}_{bulk}} \qquad (8)$$

Here diffusion from the grain boundaries into the grains interior determines the rate explaining the scaling ratio L^2/l^2 (time constant of the diffusion process $\propto$ (thickness)$^2\tilde{D}$).

Chemical diffusion effects can also appear as a consequence of purely electrical fields if the electrodes are not completely reversible for both ions and electrons [26]. This is the basis of one of the most important electrochemical methods to separate ionic and electronic conductivities, but can also be the cause of device degradation during electrical load [27].

In many cases in particular if the high temperature regime is left, the surface reaction becomes rate limiting. In this case the profiles (see Fig. 5) are horizontal and allow the determination of effective rate constants. Their interpretation depends on the rate limiting step and is -- besides other contributions -- averaging over its forward and backward rate constants. The sensitivity of the kinetics with respect to special surface treatment is obvious from Fig. 9.

V. Discussion of Some Selected Applications

Pure ion conductors are used as solid electrolytes in batteries as $ZrO_2(Y_2O_3)$ in high temperature solid oxide fuel cells allowing the transformation of the free combustion energy of H_2, of natural gas or of CH_3OH into electrical energy with high efficiency.

Solid sodium ions conductors have been discussed as electrolytes in high performance batteries using liquid Na as anode. Advantages and disadvantages of solid electrolytes become obvious with this example: The mechanical stability of the solid state allows structuring, mechanical stability as well as the use of liquid electrodes. On the other hand, it is exactly this rigidity (liquid electrodes) which causes crack formation or interfacial problems if solid electrodes are used.

Solid electrolytes can also be used for potentiometric gas sensors (e.g. $ZrO_2(Y_2O_3)$ in the λ-probe), as Na_2O-β-Al_2O_3 or Nasicon in the fast CO_2 sensor [28] characterised

by the phase scheme

$$O_2, CO_2, Na_2CO_3 \mid Na^+\text{-conductor} \mid TiO_2, Na_2Ti_6O_{13}, O_2.$$
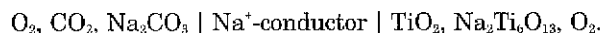
Its major advantage compared to competing electrochemical CO_2-sensors is besides of its excellent performance the possibility of exposing the open cell to atmosphere and the independence of the signal from P_{O2}.

Taguchi-type gas sensors rely on electronic conductivity. By those sensors redox-active gases, e.g. O_2 can be detected at reasonably low temperatures. Under those conditions the point defects in the solid (e.g. SnO_2) are not mobile enough (e.g. $V_O^{..}$ in SnO_2) to allow O_2 to be incorporated. Thus it stays adsorbed on the surface and traps e^- out of the space charge regions (see e.g. [29]). The subsurface of n-type is depleted and exhibits an increased resistance which depends on P_{O2}. The non-zero ionic conductivity leads to drift-effects $(\tilde{D}\neq 0)$.

Analogously the surface conductivity changes of ionic conductors can be used to detect acid-base active gases [30], e.g. NH_3 by its influence on AgCl (trapping of Ag^+) as introduced in Ref. [31].

If ionic and electronic conductivities are simultaneously of importance, i.e. if mixed conductors are involved, the ambipolar conductivity $\tilde{\sigma}$ and the chemical diffusion coefficient $\tilde{D}$ are usually high enough to allow for a fast transport of components, e.g. O in oxides. Besides the applicability in form of a bulk conducting sensor, this enables a rather selective permeation of oxygen in oxides as employed in chemical filters. In the same way the performance of electrodes, as in doped $LaCoO_3$ for solid oxide fuel cells, or TiS_2 as cathode in rechargeable Li-batteries, is improved. Conventional electrodes such as doped $LaMnO_3$ are mostly surface active, i.e. the three phase boundaries gas, electrode, electrolyte are the relevant centers for the electrochemical reaction.

$LaCrO_3$ serves as a connecting material in SOFC due to its high electronic conductivity and its reasonable environmental stability. In the same context, high temperature superconductors are of significance as loss-free conductors in the superconducting state. Mixed conductors are also of prime interest as calatyst for chemical reactions as oxygenation or hydrogenation (dehydrogenation) of hydrocarbons. Here the availability and mobility of relevant electronic and ionic centers are decisive. In some cases the catalytic activity can be enhanced by an applied voltage. Then also purely ionic materials are of interest [32].

Further applications of electroceramics concern insulators, varistors, capacitors, switching elements, magnets and actuators, to mention only a few of them (Fig. 10). In all cases defect chemistry plays a major role. To stress it again, point defects are also relevant for functional ceramics with non-electrical functions, examples are the thermal conductivity in AlN ($O_N^.$ -defects), but also preparation and corrosion of mechanical ceramics. In all cases it is the internal chemistry in bulk and boun-
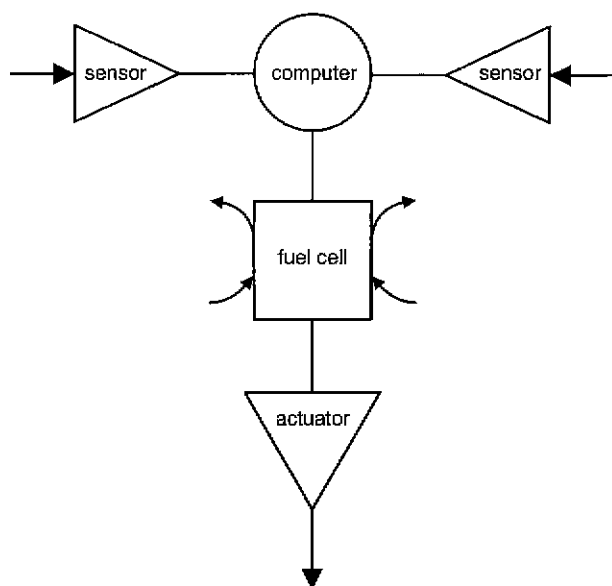
Fig. 10. The figure shows an autonomous system in which -- fed by electrochemical "metabolism" (e.g. fuel cell) -- information on the environment is obtained by senses (sensors), processed in a central "brain" (computer), and in which "motoric organs" (actuators) serve for motion and for influencing the environment. For all "organs" functional materials are of key interest.

daries as well as the chemical environment which governs the phenomena discussed here.

References

1. J. Maier, *Angew. Chem.* **105**(3), 333 (1993).

2. C. Wagner, W. Schottky, *Z. Physik. Chemie* **B11**, 163 (1930).

3. F. A. Kröger, H. J. Vinck in : *Solid State Physics* **Vol. 3**, eds. F. Seitz and D. Turnbull (Academic Press, New York, 1959).

4. G. M. Choi, H. L. Tuller, M. J. Tsai, Nato ASI Series **276**, 451 (1989).

5. J. Denk, W. Münch and J. Maier, *J. Am. Ceram. Soc.* **78**(12), 3265 (1995).

6. M. Quilitz and J. Maier, *Radiation Effects and Defects in Solids* **137**, 327 (1995); J. Maier and G. Pfundtner, *Adv. Mat.* **30**(6), 292 (1991); J. Maier and H. L. Tuller, *Phys Rev.* B **47**(13), 8105 (1993).

7. J. Maier, *Prog. in Solid St. Chem.* **Vol. 23**(3), 171 (1995).

8. C. Wagner, *Ber. Bunsenges. Phys. Chem.* **70**, 781 (1996); H. Iwahara, T. Esuka, H. Uchida, N. Maeda, *Solid State Ionics* **3/4**, 359 (1981); K.-D. Kreuer, *Chem. Mater.* **8**, 610 (1996).

9. J. Daniels, K.-H. Härdtl, D. Hennings, R. Wernicke, *Philips Res. Reps.* **31**, 487 (1976); R. Waser, *J. Am. Ceram, Soc.* **74**(8), 1934 (1991); N. H. Chan, R. K. Sharma, D. M. Smyth, *J. Electrochem. Soc.* **128**(8), 1762 (1981); E. K. Chang, A. Mehta, D. M. Smyth, *Proc. Symp. Electro-*

Ceramics and Solid State Ionics 35 (1988).

10. A. B. Lidiard in : *Handbuch der Physik* **Vol. 20**, ed. S. Fl ügge (Springer, Berlin, 1957) p. 246; *Phys. Rev.* **94**, 29 (1954).

11 N. Hainovsky and J. Maier, *Phys. Rev.* B **51**(22), 15789 (1995).

12. J. Fleig, J. Maier, *Solid State Ionics* **94**, 199 (1997).

13. M. Kleitz, H. Bernard, E. Fernandez and E. Schouler in : *Advances in Ceramics* Vol. 3, Science and Technology of Zirconia. eds. A. H. Heuer and L. W. Hobbs (The Am. Ceram. Soc., Washingto, D. C., 1981) p 310.

14. J. Maier, *Ber. Bunsenges. Phys. Chem.* **90**, 26 (1986).

15. H. Böttger, V. V. Bryksin, *Hopping Conduction in Solids* (VCH, Weinheim, 1985); A. Bunde, W. Dieterich, E. Roman, *Solid State Ionics* **18/19**, 147 (1986).

16. U. Lauer and J. Maier, *Ber. Bunsenges. Phys. Chem.* **96**, 111 (1992); S. Havlin and A. Bunde in : *Fractals and Disordered Systems*, eds. A. Bunde, S. Havlin (Springer, Berlin, 1996) p. 116, 150.

17. J. Maier, S. Prill and B. Reichert, *Solid State Ionics* **28-30**, 1465 (1988).

18. H Schmalzried, *Chemical Kinetics of Solids* (VCH, Weinheim, 1995).

19. L. Heyne in : *Solid Electrolytes*, ed. S. Geller (Springer Verlag, Berlin, 1977).

20. J. Maier, *J. Am. Ceram. Soc.* **76**(5), 1212 (1993); **76**(5), 1218 (1993); **76**(5), 1223 (1993); **76**(5), 1228 (1993).

21. I. Denk, U. Traub, F. Noll and J Maier, *Ber. Bunsenges. Phys Chem,* **99**(6), 798 (1995).

22. T Bieger, J. Maier and R. Waser, *Ber. Bunsenges. Phys. Chem.* **97**(9), 1098 (1993); I. Denk, F. Noll and J. Maier, *J. Am. Ceram. Soc.*, in press; H,-J. Schlüter, M Barsoum and J. Maier, *Solid State Ionics.* in press; Ch. Tragut, Dissertation, Universität Karlsruhe, 1992.

23. T. Bieger. H. Yugami, N. Nicoloso, Joachim Maier and R. Waser, *Solid State Ionics* **72**, 41 (1994); R. I. Merino, N. Nicoloso, J. Maier, in : *Ceramic Oxygen Ion Conductors and Their Technological Applications*, ed. B. C. H. Steele, The University Press Cambridge (1996), pp. 43-52.

24. J. Jamnik and J. Maier, *Ber. Bunsenges. Phys. Chem.* **101**(1), 23 (1997); *J. Electrochem. Soc* , submitted.

25. W. Preis and W. Sitte, *J. Appl. Phys.* **79**, 1 (1996).

26. C. Wagner in : *Progress in Solid State Chemistry* **6**, ed. H. Reiss (Pregamon Press, Oxford, 1971); J. Maier, *Solid State Phenomena* **39-40**, 35 (1994).

27. R. Waser, T. Baiatu, K.-H. Härdtl, *J. Am. Ceram. Soc.* **73**(6), 1645 (1990).

28. M. Holzinger, J. Fleig, J. Maier and W. Sitte, *Ber. Bunsenges. Phys. Chem.* **99**(11), 1427 (1995).

29. W. Göpel. *Progr. Surf. Sci.* **20**, 1 (1986).

30. J. Maier, *Solid State Ionics,* **62**, 105 (1993).

31. J. Maier, in : *Recent Trends in Superionic Solids and Solid Electrolytes* (S. Chandra, A. Laskar (eds.)), Academic Press, New York (1989), pp. 137.

32. C. G. Vayenas, S. Bebelis, I. V. Yentekakis and H. G. Lintz, *Catalysis Today* **11**, 303 (1992).